Mixing and matching TREK/TRAAK subunits generate heterodimeric K_{2P} channels with unique properties

Sandy Blin[a], Ismail Ben Soussia[a], Eun-Jin Kim[b], Frédéric Brau[a], Dawon Kang[b,1], Florian Lesage[a,1], and Delphine Bichet[a]

[a]Institut de Pharmacologie Moléculaire et Cellulaire, Laboratoire d'Excellence Canaux Ioniques d'Intérêt Thérapeutique, CNRS, Université de Nice Sophia Antipolis, 06560 Valbonne, France; and [b]Department of Physiology, College of Medicine and Institute of Health Sciences, Gyeongsang National University, Jinju 660-751, South Korea

Edited by Lily Yeh Jan, University of California, San Francisco, CA, and approved February 23, 2016 (received for review November 17, 2015)

The tandem of pore domain in a weak inwardly rectifying K^+ channel (Twik)-related acid-arachidonic activated K^+ channel (TRAAK) and Twik-related K^+ channels (TREK) 1 and TREK2 are active as homodimers gated by stretch, fatty acids, pH, and G protein-coupled receptors. These two-pore domain potassium (K_{2P}) channels are broadly expressed in the nervous system where they control excitability. TREK/TRAAK KO mice display altered phenotypes related to nociception, neuroprotection afforded by polyunsaturated fatty acids, learning and memory, mood control, and sensitivity to general anesthetics. These channels have emerged as promising targets for the development of new classes of anesthetics, analgesics, antidepressants, neuroprotective agents, and drugs against addiction. Here, we show that the TREK1, TREK2, and TRAAK subunits assemble and form active heterodimeric channels with electrophysiological, regulatory, and pharmacological properties different from those of homodimeric channels. Heteromerization occurs between all TREK variants produced by alternative splicing and alternative translation initiation. These results unveil a previously unexpected diversity of K_{2P} channels that will be challenging to analyze in vivo, but which opens new perspectives for the development of clinically relevant drugs.

potassium channel | subunit assembly | electrophysiology | pharmacology | heteromerization

Tandem of pore domain in a weak inwardly rectifying K^+ channel (Twik)-related K^+ channels (TREK) 1, TREK2, and Twik-related acid-arachidonic activated K^+ channel (TRAAK) channels produce inhibitory background K^+ currents (1–3). These channels respond to neuroprotective fatty acids, mechanical stretch, temperature, pH, and neurotransmitters through G protein-coupled receptors (GPCRs) (for a recent review, see ref. 4). TREK1 is activated by volatile anesthetics and plays a role in general anesthesia. These channels have emerged as promising targets for the development of other classes of clinical compounds. TREK1 is activated by opioid receptors and contributes to morphine-induced analgesia, but is not involved in morphine-induced constipation, respiratory depression, and dependence (5). TREK1 openers, acting downstream from opioid receptors, might have strong analgesic effects without adverse effects (6). TRAAK may also be a good target for analgesia: Its activation by angiotensin II receptors is responsible for the painless nature of the early lesions of the necrotizing tropical disease Buruli ulcer (7). Also, activation of TREK1 by $GABA_B$ receptors in the hippocampus (8), and inhibition of TREK2 by neurotensin receptors in the entorhinal cortex (9), suggests that specific modulators of these channels might also have beneficial actions against drug abuse, and against learning slow down and memory deficits in Alzheimer's disease. Finally, inhibition of TREK1 by spadin (10), an endogenous peptide, or by the antidepressant fluoxetine (Prozac) (11), pinpoints it as a valuable target for the treatment of depression. TREK/TRAAK channels are broadly expressed in the nervous system (12–15). TREK1 is more specifically expressed in the striatum, TREK2 in the cerebellum, and TRAAK in the thalamus. All of the subunits are coexpressed in the cortex, hippocampus, hypothalamus, amygdala, and olfactory system (12), and in the spinal cord (16, 17).

K_{2P} channels are dimers of subunits (18–20). Heterodimerization has been shown to occur between the members of two subfamilies of K_{2P} channels: the TASK (21) and THIK (22) channels. Heterodimerization of TREK1 with TWIK1 has been proposed to generate glutamate-permeant channels in astrocytes (23). Because TREK/TRAAK subunits show an overlapping distribution in many areas of the nervous system and because heteromerization produces channels with unique electrophysiological and pharmacological properties, we evaluated their ability to form active heterodimers. Because alternative splicing (AS) (1, 24) and alternative translation initiation (ATI) (25, 26) increase TREK diversity, we also tested heterodimerization between the different AS and ATI variants of TREK1 and TREK2, and we reevaluated heteromerization of TREK1 with TWIK1.

Results

Assembly of TREK/TRAAK Subunits in Mammalian Cells. Coexpression and colocalization of TREK1, TREK2, and TRAAK in dorsal root ganglia (DRG) neurons suggested that they can form heterodimers in vivo (Fig. S1 *A* and *B*). Thus, we studied heteromerization of TREK1, TREK2, and TRAAK in transfected MDCK cells. Colocalization of TREK1 with TREK2 or TRAAK is illustrated in Fig. 1*A*. Furthermore, TREK2 and TRAAK coprecipitated with TREK1 from these cells (Fig. 1*B* and Fig. S1*C*). We next demonstrated protein interaction by Förster/fluorescence resonance energy transfer (FRET) and Duolink in situ proximity ligation

Significance

Nearly 350 human genes encode ion channels. Posttranscriptional (alternative splicing, editing, and alternative translation initiation) and posttranslational mechanisms (glycosylation, phosphorylation) further increase diversity. For multimeric channels, various heteromeric combinations may raise the number of ion channels to thousands. Here, we show that mixing and matching TWIK1-related K^+ (TREK)/Twik-related acid-arachidonic activated K^+ channel (TRAAK) subunits generate tens of different channels. Heterodimeric combinations have properties different from those of the corresponding homodimers, including single-channel behavior, regulation by kinases, and sensitivity to pharmacological agents. These results imply that any excitable cell can adjust its response to neurotransmitters by simply modulating the ratio of expressed TREK/TRAAK subunits. These results also imply that heteromerization has to be considered when analyzing in vivo functions of these channels but also when screening new potential therapeutic drugs.

Author contributions: S.B., I.B.S., E.-J.K., D.K., F.L., and D.B. designed research; S.B., I.B.S., E.-J.K., D.K., and D.B. performed research; F.B. contributed new reagents/analytic tools; S.B., I.B.S., E.-J.K., D.K., F.L., and D.B. analyzed data; and S.B., I.B.S., E.-J.K., D.K., F.L., and D.B. wrote the paper.

The authors declare no conflict of interest.

This article is a PNAS Direct Submission.

[1]To whom correspondence may be addressed. Email: lesage@ipmc.cnrs.fr or dawon@gnu.ac.kr.

This article contains supporting information online at www.pnas.org/lookup/suppl/doi:10.1073/pnas.1522748113/-/DCSupplemental.

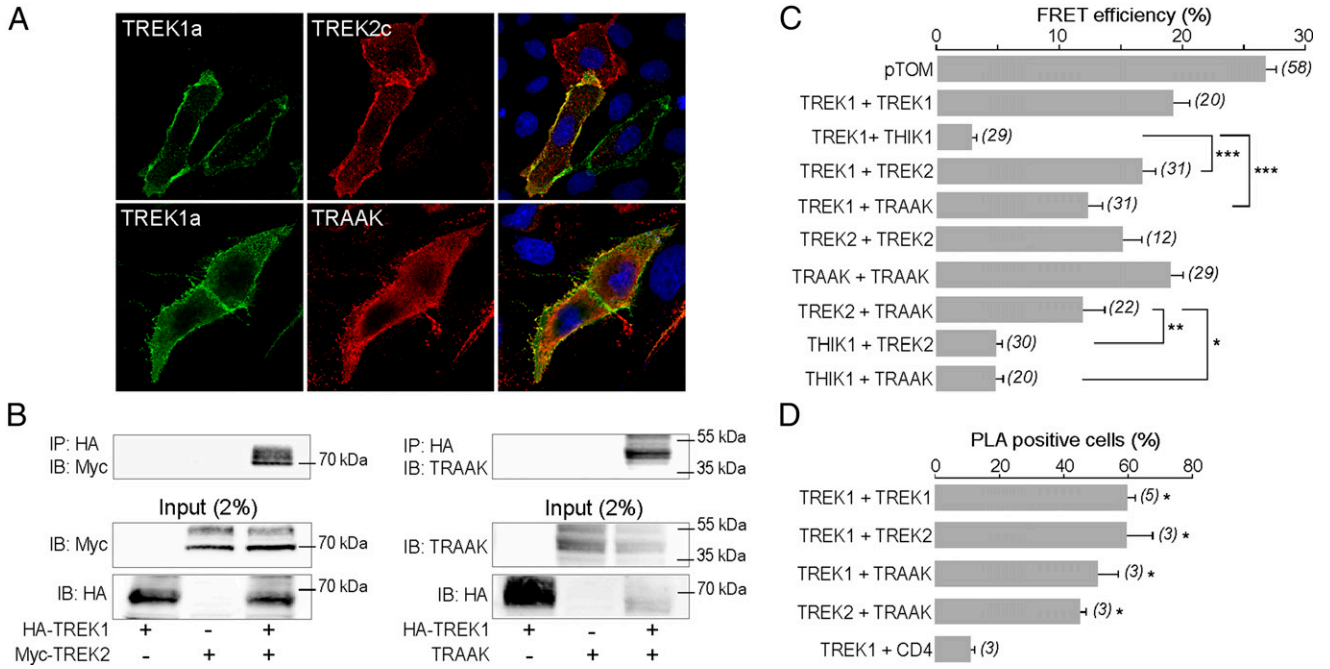

Fig. 1. TREK1, TREK2, and TRAAK interact in transfected MDCK cells. (*A*) Immunolocalization of HA-TREK1a (green) and Myc-TREK2c (red) or TRAAK (red). (*B*) Coimmunoprecipitation experiments. Inputs represent 2% of the total cell lysate. (*C*) FRET experiments. Different combinations of TREK1, TREK2, TRAAK, and THIK1 fused to enhanced cyan fluorescent protein (eCFP) and enhanced yellow fluorescent protein (eYFP) were coexpressed. eCFP directly linked to eYFP in pTOM serves as positive control. FRET was measured at the plasma membrane. Number of cells is given in parentheses. Data were analyzed by using one-way ANOVA with post hoc multiple comparisons using the Tukey's test: $*P < 0.05$, $**P < 0.01$, and $***P < 0.001$. (*D*) Duolink in situ PLA. Percentage of cells corresponds to the number of PLA-positive cells relative to the number of transfected cells. Number of independent experiments is given in parentheses and corresponds to >300 cells analyzed. Mann–Whitney test versus TREK1+CD4 as negative control: $*P < 0.05$.

assay (PLA). Both techniques rely on the close proximity between two interacting proteins (<40 nm for PLA and <10 nm for FRET). Quantitative and statistical analysis of the FRET efficiency is given in Fig. 1*C* for various combinations of subunits. In TREK1-expressing cells, positive FRET signals were observed with TREK1 (19.2 ± 1.7%), TREK2 (15.1 ± 1.7%), and TRAAK (12.3 ± 1.3%), but not with THIK1 (2.8 ± 0.6%). Similar data were obtained for TREK2 and TRAAK, demonstrating that all combinations of TREK/TRAAK subunits are able to produce FRET in transfected cells. FRET efficiency seems to be lower between TRAAK and TREK1 or TREK2, than between TREK1 and TREK2. This difference might reflect a lower affinity between TRAAK and TREK1 or TREK2, than between TREK1 and TREK2. These results were confirmed by PLA using tagged subunits (Fig. 1*D*). Positive signals were observed in a high percentage of cells coexpressing TREK1 with TREK1 (60.1 ± 2.6%), TREK2 (60 ± 8%), or TRAAK (50.8 ± 6.6%), significantly different from cells coexpressing TREK1 with CD4 (11.5 ± 1.2%).

TREK/TRAAK Subunits Do Not Assemble with Other K_{2P} Subunits. We next tested a potential assembly of TREK1 with more distant members of the K_{2P} channel family (Fig. 2*A*). Quantification of the PLA signal is given in Fig. 2*B* and compared with positive (TREK1, 60.1 ± 2.6%) and negative (CD4, 11.5 ± 1.2%) controls. TASK1 (4.8 ± 0.9%), TASK3 (6.3 ± 2.7%), and TWIK-related alkaline sensitive K^+ channel (TALK) 1 (6.9 ± 2%) gave lower signals than CD4, whereas signals for THIK1 (20.8 ± 0.8%), TALK2 (15.9 ± 3.1%), TWIK-related spinal cord K^+ channel (TRESK) (16.9 ± 3.6%), and TWIK1 (21.2 ± 8.8%) were higher than CD4 but significantly lower than that for TREK1 (60.1 ± 2.6%). All tested K_{2P} subunits are correctly expressed at the cell surface except TWIK1, which is mainly localized to endosomes (27) (Fig. S2*A*). The lack of colocalization or coimmunoprecipitation between TREK1 and TWIK1 further confirms the absence of interaction (Fig. S2 *A* and *B*). We also tested a mutant of TWIK1 expressed at the plasma membrane (TWIK1 $I_{293}A$, $I_{294}A$ noted TWIK1*). The expression of TWIK1* instead of TWIK1 did not favor interaction with TREK1 in the PLA assay (Fig. 2*B*) nor increases coimmunolocalization in cells coexpressing TREK1 and TWIK1* (Fig. S2*A*). Again, FRET was unable to show any evidence of assembly between TREK1 and TWIK1* (Fig. S2*C*). Together, the results show that multimerization is restricted to

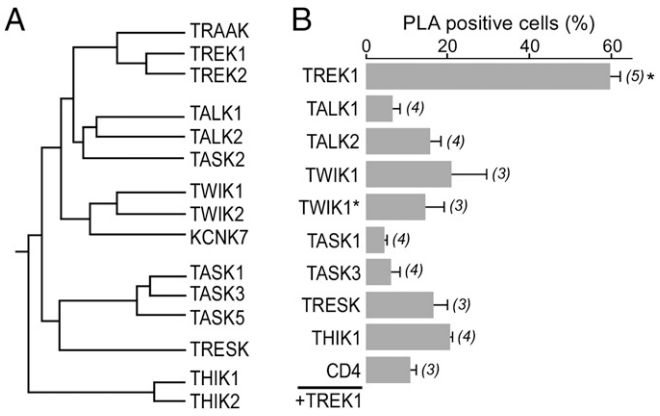

Fig. 2. Assembly is restricted between the members of the TREK/TRAAK subfamily. (*A*) Phylogenetic tree of human K_{2P} subunits. The tree was constructed with a multiple alignment using fast Fourier transform (MAFFT) program. (*B*) Duolink in situ PLA between TREK1 and other K_{2P} subunits representative of the different subfamilies. HA-TREK1 was coexpressed in MDCK cells with Myc-tagged subunits. Percentage of positive cells corresponds to the number of PLA-positive cells relative to the number of transfected cells. Number of independent experiments is given in parenthesis and corresponds to >300 cells analyzed per condition. Data were analyzed by using Mann–Whitney test: $*P < 0.05$ versus TREK1+CD4 as negative control.

members of the TREK/TRAAK subfamily and does not extend to other K_{2P} channel subunits.

All Variants of TREK1 and TREK2 Assemble. In the above experiments, TREK1a and TREK2c isoforms were used to demonstrate TREK1/TREK2 assembly. We next wondered whether other isoforms of TREK1 and TREK2 produced by AS and ATI form heterodimers. All TREK1 isoforms were tagged and coexpressed with TREK2c (Fig. 3*A* and Fig. S3). Similarly five known TREK2 isoforms were tagged and coexpressed with TREK1a (Fig. 3*B*). All of the combinations tested generated strong PLA signals (>70% of positive cells) compared with negative control (<3% for the empty vector) (Fig. 3 and Fig. S3).

TREK/TRAAK Assemblies are Heterodimeric Channels. If heterodimers form between TREK and TRAAK, then each monomer contributes to the ionic pore. To discriminate between aggregates of TREK and TRAAK homodimers and TREK/TRAAK heterodimers, we replaced the first glycine of the G(Y/L/F)G signature sequence with a glutamate in the pore loop of the TRAAK subunit producing a nonconducting dimer when the subunit is expressed alone or a dominant-negative subunit when it assembles with the corresponding wild-type subunit (22). $TRAAK^{DN}$ (TRAAK $G_{106}E$) was coexpressed with wild-type subunits in *Xenopus* oocytes (Fig. 4*A*). Typical currents and mean current values are respectively illustrated in Fig. S4*A* and Fig. 4*A*. The current amplitude in oocytes coexpressing TRAAK and $TRAAK^{DN}$ is 41 ± 0.03% of the value obtained for TRAAK alone. By expressing three times more $TRAAK^{DN}$ than TRAAK, active dimeric TRAAK channels should only represent 6.25% of the total population of channels. $TRAAK^{DN}$ silences 59% of the current instead of the expected 93.75%, suggesting that the affinity between $TRAAK^{DN}$ and TRAAK is lower than that between TRAAK and TRAAK, or that $TRAAK^{DN}$ is not processed as effectively as TRAAK. Although incomplete, the dominant-negative effect of $TRAAK^{DN}$ was tested on TREK1, TREK2, and THIK1. $TRAAK^{DN}$ inhibited TREK1 (56% of inhibition) and TREK2 (66%), significantly more than THIK1 (18%) (Fig. 4*A*). Similar observations were made by using $TREK1^{DN}$ (Fig. S4*B*). Whereas $TREK1^{DN}$ was able to inactivate 49%, 32%, and 57% of the TREK1, TREK2, and TRAAK currents, respectively, it had only a weak effect on THIK1 (14%), TWIK1 (9%), and TASK3 (5%) (Fig. S4*B*).

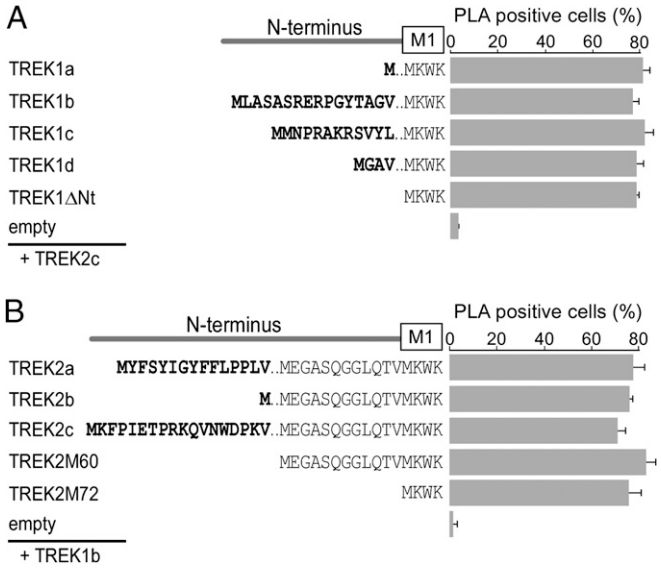

Fig. 3. TREK1 and TREK2 isoforms assemble in MDCK cells. (*A*) TREK1 isoforms produced by AS of exon 1, TREK1a, b, c, and d, or by ATI, TREK1ΔNt, were coexpressed with TREK2c isoform and used for PLA measurements. Quantitative measurement is illustrated by a bar graph with the partial N-ter aa sequences of the various mouse TREK1 isoforms. MKWK sequence is the beginning of the first membrane-spanning domain M1. The gap in the N-ter corresponds to 40 residues. (*B*) TREK2 variants generated by AS (TREK2a, b, and c) or ATI (TREK2M60, M72, starting at methionine 60 or 72 numbered from TREK2c) were coexpressed with TREK1b. PLA quantification is given with the N-ter sequences of the various mouse TREK2 isoforms. The gap in the N-ter corresponds to 36 residues. Three independent experiments were performed that correspond to >250 cells analyzed per condition.

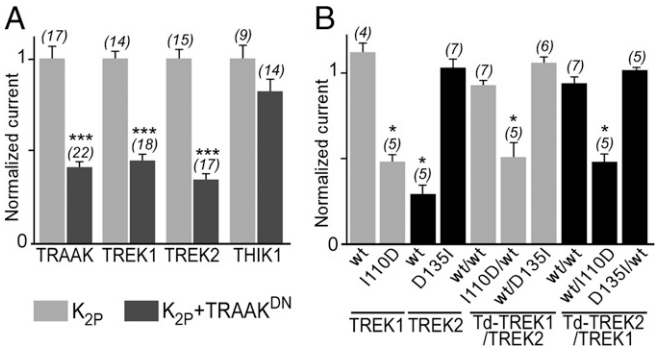

Fig. 4. Contribution of each TREK/TRAAK monomer to the formation of heterodimers. (*A*) Dominant-negative TRAAK mutant bearing a loss of function mutation ($TRAAK^{DN}$, TRAAK G106E) in the first pore domain was coexpressed with TRAAK, TREK1, TREK2, and THIK1 in oocytes (3:1 ratio, 7.5 ng/2.5 ng) and current recorded at membrane potentials ranging from −120 mV to +60 mV from a holding potential of −80 mV in 10-mV increments. Histograms represent normalized current at 0 mV for oocytes expressing K_{2P} subunit alone (gray) or with $TRAAK^{DN}$ (black). Two-sample *t* test: ***$P < 0.001$. (*B*) RR sensitivity of TREK1, TREK2, and covalent TREK1/TREK2 tandems (Td-TREK1/TREK2 and Td-TREK2/TREK1). I110D and D135I substitution correspond to mutation of the RR binding site in mouse TREK1a or TREK2c. Each cRNAs were injected alone in oocytes; currents were elicited as in *A*. For normalized current values, current measured at −100 mV in 80 mM K^+ solution after addition of 10 μM RR was compared with current obtained in 80 mM K^+ solution (control) and analyzed with paired Wilcoxon test: *$P < 0.05$. Number of oocytes is given in parentheses.

We further demonstrated the contribution of both TREK1 and TREK2 subunits to the formation of an active heterodimer by manipulating a binding site for ruthenium red (RR) (Fig. 4*B*). TREK2 is inhibited by external application of RR but not TREK1 (28). Sensitivity to RR is afforded by charged residues close to the external mouth of the ionic pore (21). In TREK2, this residue is aspartate 135, which is replaced by isoleucine 110 in RR-insensitive TREK1. To express pure heterodimers, we engineered constructs for expression of covalent tandems in which two subunits are concatenated into a single polypeptide. Tandems of TREK1 and TREK2 are noted Td-TREK1/TREK2 or Td-TREK2/TREK1, depending on the order of each subunit in the dimer. As expected, TREK2 and Td-TREK2/TREK2 are sensitive to RR, whereas TREK1 and Td-TREK1/TREK1 are not affected (Fig. 4*B* and Fig. S5). Replacing aspartate 135 by an isoleucine (D135I) in TREK2 abolishes its sensitivity to RR, whereas replacing isoleucine 110 by an aspartate (I110D) into TREK1 confers RR sensitivity. Td-TREK1/TREK2, Td-TREK1/$TREK2_{D135I}$, Td-TREK2/TREK1, and Td-$TREK2_{D135I}$/TREK1 that contain only one or no aspartate residue are insensitive to RR. Introducing I110D into the TREK1 moiety bestows RR sensitivity to Td-$TREK1_{I110D}$/TREK2 and Td-TREK2/$TREK1_{I110D}$. This result further demonstrates that each TREK moiety contributes to the formation of the active pore.

Heterodimers of TREK/TRAAK Subunits Have Their Own Electrophysiological and Pharmacological Characteristics. Cell-attached patch recordings from HEK293 cells expressing TREK1, TREK2, or Td-TREK1/TREK2 display typical single-channel openings (Fig. 5). In agreement with earlier studies, TREK1 and TREK2 exhibit different behaviors (29). TREK1 conducts more outward currents at +100 mV than at −100 mV (outward rectification), whereas TREK2 shows

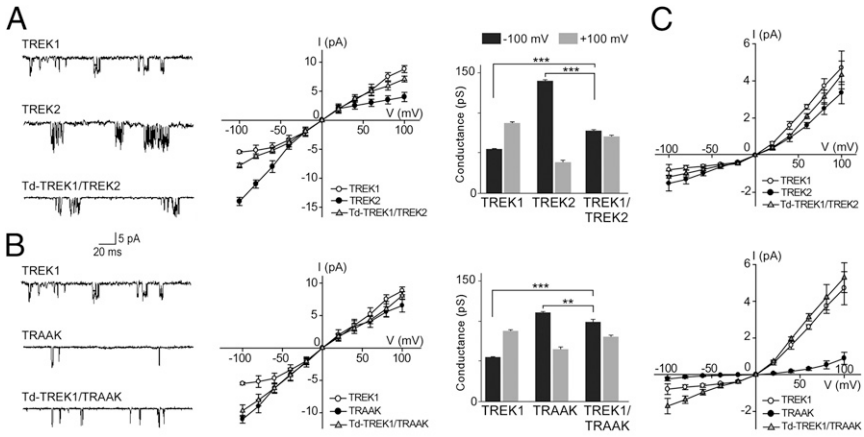

Fig. 5. Single-channel properties of TREK/TRAAK homomeric and heteromeric channels in transfected HEK293 cells. (*A*) Electrophysiological properties of TREK1, TREK2 and Td-TREK1/TREK2. (*Left*) Single-channel recordings at −60 mV. Currents were recorded in cell-attached patches held at pipette potentials from +100 mV to −100 mV in bath solution containing 150 mM KCl. (*Middle*) Single-channel current–voltage relationships (n = 10). (*Right*) Unitary conductances at −100 and +100 mV (n = 10). (*B*) Electrophysiological properties of TREK1, TRAAK, and Td-TREK1/TRAAK. (*Left*) Single-channel recordings from cells expressing TREK1, TRAAK, and Td-TREK1/TRAAK at −60 mV. Currents were recorded as in *A*. (*Middle*) Single-channel current–voltage relationships of the different channels (n = 10). (*Right*) Unitary conductances at -100 and +100 mV (n = 10). (*C*) Current–voltage relationships of mean currents. The mean currents (I = NPoi) were obtained from cell-attached macropatches (n = 5). Mann–Whitney test: $^{**}P < 0.01$ and $^{***}P < 0.001$.

the opposite behavior (inward rectification) (Fig. 5*A*). Td-TREK1/TREK2 is different from TREK1 and TREK2 and has a linear current-voltage (IV) relationship (no rectification). Unitary conductances of TREK1, TREK2, and Td-TREK1/TREK2 are 88.5 ± 6.2 pS, 39.8 ± 2.8 pS, and 71.6 ± 2 pS at +100 mV and 55.6 ± 0.6 pS, 140.9 ± 2 pS, and 78.9 ± 1.3 pS at −100 mV, respectively (n = 10). Fig. 5*B* shows single-channel openings of TREK1, TRAAK, and Td-TREK1/TRAAK at a pipette potential of −60 mV. The IV relationship of Td-TREK1/TRAAK is similar to that of TRAAK. Unitary conductances of TRAAK and Td-TREK1/TRAAK are 65.4 ± 3.2 pS and 80.7 ± 1.9 pS at +100 mV and 110.9 ± 1.5 pS and 98.7 ± 3.9 pS at −100 mV, respectively (n = 10). Unpredictably, heteromeric channels have intermediate unitary conductances compared with each homomeric channel (Fig. 5 *A* and *B*). Mean currents in symmetrical 150 mM KCl, which reflect the product of open probability and single-channel conductance, are shown in Fig. 5*C*.

We next investigated Td-TREK1/TRAAK sensitivity to potential therapeutic compounds such as ML67 and fluoxetine (Fig. 6 *A* and *B*). ML67, a carbazole-based molecule, has been recently identified as a potent activator of TREK1 currents in a high-throughput screening assay (30). In HEK293 cells, TREK1,

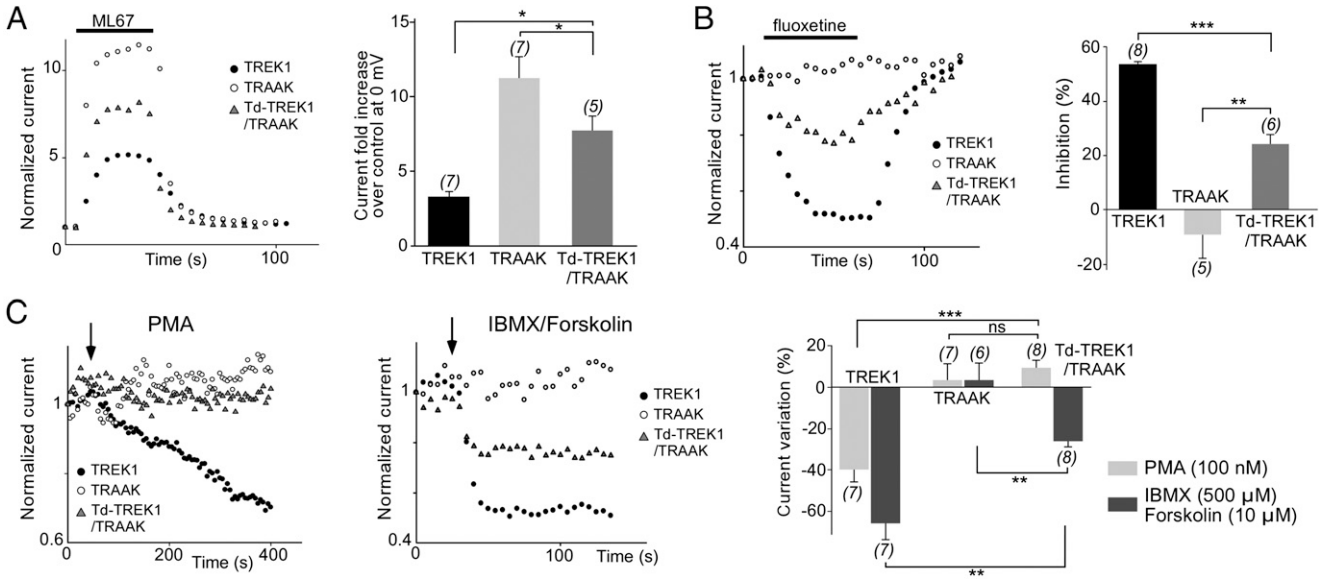

Fig. 6. Pharmacology and regulation of heteromeric TREK1/TRAAK channels in transfected HEK293 cells. (*A*) Effect of ML67 on TREK1, TRAAK, and Td-TREK1/TRAAK. (*Left*) Kinetics of current amplitude at 0 mV for each construct during application of ML67 (100 μM) (black bar) normalized to currents at t = 0 s. (*Right*) Current fold increase under ML67 application at 0 mV. (*B*) Effect of fluoxetine on TREK1, TRAAK, and Td-TREK1/TRAAK. (*Left*) Kinetics of current amplitude at 0 mV during application of 10 μM fluoxetine (black bar) were normalized to currents at t = 0 s. (*Right*) Percentage of current inhibition induced by fluoxetine at 0 mV. (*C*) Regulation of TREK1, TRAAK, and Td-TREK1/TRAAK by kinases. PMA (100 nM) or IBMX/Forskolin (500 μM/10 μM) were applied to activate protein kinase C or protein kinase A. (*Left* and *Middle)* Current kinetics at 0 mV before and after application of PMA or IBMX/Forskolin (arrow) were normalized to currents at t = 0 s. (*Right*) Current variations were determined by comparing currents at 0 mV with or without drugs. Mann–Whitney test: $^{**}P < 0.01$, $^{***}P < 0.001$, and ns is not significant. Number of cells is given in parentheses.

TRAAK, and Td-TREK1/TRAAK are all largely activated by ML67, but with different intensities. TREK1 current was increased by 3.3 ± 0.4-fold, TRAAK current by 11.3 ± 1.4-fold and Td-TREK1/TRAAK by 7.8 ± 1-fold, an intermediate activation profile (Fig. 6*A*). We also tested the effect of fluoxetine (Prozac) (Fig. 6*B*) (11). Fluoxetine had no effect on TRAAK current but inhibits TREK1. Interestingly, Td-TREK1/TRAAK displays fluoxetine sensitivity but to a lesser extent than TREK1 (24.4 ± 3.5% of current inhibition versus 53.6 ± 1.3% for TREK1) (Fig. 6*B*).

Regulation of Td-TREK1/TRAAK by protein kinase A (PKA) and C (PKC) were also investigated in HEK293 cells. As previously reported and illustrated in Fig. 6*C*, TREK1 currents are largely inhibited by PKC-activator phorbol-12 myristate-acetate (PMA) (39.8 ± 6.2% of inhibition) or by stimulation of PKA by a mixture of forskolin and 3-isobutyl-1-methylxanthine (IBMX) (65.8 ± 7.9% of inhibition), whereas TRAAK currents are not significantly affected by these compounds (1, 2). In the same conditions, Td-TREK1/TRAAK currents were unaffected by PKC activation like TRAAK (9.6 ± 3.7% of stimulation) but inhibited by PKA activation like TREK1 (25.9 ± 3.2% of inhibition). Similar results were obtained by using Td-TREK1/TREK1, Td-TRAAK/TRAAK, and Td-TRAAK/TREK1, indicating that the covalent fusion of the two subunits does not affect channel function and regulations (Fig. S6).

Discussion

Unlike K_v and K_{ir} channels that form tetramers, K_{2P} channels require the assembly of two subunits to form the ion-conducting pore. The interaction between TASK1 and TASK3 was the first demonstration to our knowledge of heterodimerization between K_{2P} subunits (21). Recently, we reported an interaction between THIK1 and THIK2 (22). TASK1 and TASK3 share 49% of amino acid (aa) identity, and THIK1 and THIK2 60% of aa identity. TREK/TRAAK assembly suggests that K_{2P} subunits sharing at least 30% of aa identity (i.e., belonging to the same subfamily) are prone to form heterodimers. Assembly efficacy increases with sequence conservation as we observed a better association of TREK1 with TREK2 (47% of aa identity) than with TRAAK (31% of aa identity). In contradiction with a previous study (23), we found no interaction between TREK1 and TWIK1 (24% of aa identity). Another study failed to demonstrate TREK1/TWIK1 interaction by using FRET in CHO cells (31). Finally, it has also been suggested that TWIK1 may interact with TASK1 and TASK3, providing another example of assembly between members of distant subfamilies (TWIK1 sharing less than 22% of aa identity with TASK1 and TASK3) (31). However, these results have not yet been reproduced by another laboratory. More studies are clearly needed to explore a potential interaction between K_{2P} subunits belonging to distinct subfamilies.

Mechanisms controlling K_{2P} assembly are unresolved even if we have shown that the extracellular loop between the first membrane spanning segment and the first pore domain is able to interact with another identical loop (20). Cytoplasmic N-terminals of K_v and K_{ir} channels are involved in tetramerization (32, 33). Furthermore, a domain called T1 in the N-ter of K_v channels sets the compatibility of different subunits for heteromerization (34). The lack of the cytoplasmic N-ter does not prevent interaction between short TREK1 (TREK1ΔNt) or TREK2 (TREK2M60 and TREK2M72) variants (Fig. 3). Although the N-ter might initiate priming contact between subunits and contribute to intersubunit stability, its integrity does not seem critical for K_{2P} channel assembly. However, interaction between all AS and ATI variants of TREK1 and TREK2 demonstrates that the function of AS and ATI in the TREK/TRAAK subfamily is not to limit heterodimerization between specific isoforms.

Heteromeric assembly of K^+ channel subunits is a way to increase channel diversity without increasing the number of genes. For TREK/TRAAK channels, heteromerization comes in addition to the molecular diversity generated by AS and ATI that already affect conductance (25), ion selectivity (26), and pharmacology (35). Single-channel properties of TREK1 and TREK2 channel have been extensively studied over the past decade (29). Compared with TREK2 and TRAAK, TREK1 produces outwardly rectifying currents, due to a reduced unitary conductance and bursting behavior at negative membrane potentials. Interestingly, TREK1/TREK2 heterodimers keep this property and display voltage-dependent gating and open probability similar to TREK1. On the contrary, when TREK1 is combined to TRAAK, this characteristic is lost and TREK1/TRAAK heterodimers behave as linear leak channels. Heterodimerization also impacts channel regulation. Activation of PKA has no effect on TRAAK but down-regulates TREK1 and TREK1/TRAAK. TRAAK lacks the serine residue that is phosphorylated by PKA in TREK1 (S333) and is not sensitive to PKA. Only one PKA phosphorylation site in TREK1/TRAAK heterodimer seems sufficient to provide sensitivity to PKA. The absence of effect upon PKC stimulation on TRAAK and TREK1/TRAAK is more puzzling because the substrate site for PKC identified in TREK1 (S300) is present in TRAAK (S261) and TREK1/TRAAK. A sequential phosphorylation mechanism may explain this result. In TREK1, PKC phosphorylation would be favored by prior PKA phosphorylation (29, 36). In TRAAK and TREK1/TRAAK, the absence or limited access to PKA site would render subsequent PKC modification inefficient.

In vivo, GPCR-activated metabotropic signaling pathways control PKA and PKC regulation of TREK channels. Activation of Gs-coupled serotonin (5HT4R) and noradrenaline (β2AR) receptors causes inhibition of TREK1 and TREK2 channel via a PKA-dependent phosphorylation (3, 37). In an opposite manner, stimulation of the Gi-coupled adrenergic (α2AR), glutamate (mGluR2, mGluR4), γ-aminobutyrate ($GABA_BR$) receptors activates TREK1 and TREK2 through adenylate cyclase inhibition, producing a decrease of cyclic adenosine monophosphate and PKA activity favoring channel dephosphorylation (3, 8, 38). Phosphorylation by PKC induces inhibition of TREK1 and/or TREK2 by Gq-coupled receptors through TSH releasing hormone receptor, orexin, acetylcholine (M3-R), and neurotensin (1, 15, 36). Other pathways contributing to Gq-mediated inhibition of TREK channels include mGluR1 activation through direct diacylglycerol and phosphatidic acid effects or through phosphatidylinositol 3,5-bisphosphate breakdown rather than activation of PKC (29). These regulations of TREK1 and TREK2 are important for the dynamic control of cell excitability as shown in the hippocampus and entorhinal cortex (8, 38). On the contrary, neither PKA nor PKC influences TRAAK activity (2). TRAAK has been shown to be insensitive to mGluR1 stimulation, suggesting that the channel is also insensitive to other Gq-mediated signaling pathways (39). Our results suggest that TREK1/TRAAK heterodimers display intermediate sensitivity to neurotransmitters and receptor activation. In cells coexpressing both TREK1 and TRAAK subunits, a controlled change in the TREK1:TRAAK ratio will influence the proportion of homomeric versus heteromeric channels and, therefore, the degree of the cellular response to GPCR stimulation, without requiring changes in other cellular parameters.

Recently, some efforts have been made in identifying compounds that modulate the activity of TREK/TRAAK channels. BL-1249, a fenamate-like compound, and ML67-33, a dihydroacridine analog, activate TREK1, TREK2, and TRAAK and their isoforms with various N-ter lengths (30, 35). For those compounds that are not targeting a unique TREK subunit, TREK/TRAAK heteromerization has only a moderate influence as illustrated by the intermediate sensitivity of TREK1/TRAAK heterodimers to ML67 compared with TREK1 or TRAAK homodimers. By contrast, with more specific molecules such as spadin and fluoxetine that inhibit TREK1 without affecting TREK2 or TRAAK, heteromerization increases the spectrum of action of the drug to TREK1/TRAAK heterodimers.

Conclusion

Our results unveil a previously unexpected diversity of K_{2P} channels that will be challenging to analyze in vivo, but opens new perspectives for the development of clinically relevant drugs. TREK channel modulators provide a path to novel analgesics,

anesthetics, neuroprotectors or antidepressants. Future pharmacological studies will have to take TREK/TRAAK heteromerization and the resulting diversity into account when screening drugs and studying their selectivity.

Methods

Constructs. Mouse and human channel subunits were cloned into pcDNA3 or pIRES2-eGFP for mammalian cells expression and pLIN for *Xenopus* oocyte expression. For immunocytochemistry, coimmunoprecipitation, and PLA experiments, Myc or HA tags were inserted by PCR. For FRET experiments, channel subunits were subcloned into pECFP or pEYFP vectors. All mutations were introduced by PCR using Pfu-Turbo DNA polymerase (Agilent). Heteromeric tandems were constructed by overlapping PCRs, whereas homomeric tandems were constructed by separate PCRs and cloned into appropriate vector.

MDCK Culture, Transfection, Immunocytochemistry, and Coimmunoprecipitation. Classical methods have been used that are described in *SI Methods*.

Oocyte Expression and Two-Electrode Voltage Clamp Recordings. Experiments were carried out as described in ref. 22 for dominant-negative experiments and in ref. 28 for RR sensitivity.

Electrophysiology on HEK293 Cells. HEK293 cells grown in 35-mm dish were transfected with K_{2P} channels using Lipofectamine 2000 (Invitrogen) or Jet PEI (Polyplus transfection). Cells were used 2–3 d after transfection. Electrophysiology was carried out by using classical methods described in *SI Methods*.

Duolink PLA. MDCK cells were cotransfected with a pIRES2-eGFP and a pcDNA3 construct, each containing a K_{2P} subunit. Cells were fixed, permeabilized, and incubated with primary antibodies and processed for Duolink revelation detailed in *SI Methods*. Percentage of PLA-positive cells was determined counting positive cells (red) over transfected cells (green) of 12–14 microscopic fields per transfection randomly chosen. The experiments were repeated 3–5 times, leading to more than 500 cells analyzed per condition.

FRET. MDCK cells were cotransfected with fluorescent constructs of K_{2P} subunits. FRET measurements were performed on fixed cells with a laser scanning confocal microscope (TCS SP5, Leica Microsystems) by using gradual acceptor photobleaching strategy as described in *SI Methods*. FRET efficiency was calculated by using the following formula: $(I_{max} - I_0)/I_{max}$. I_0 corresponds to CFP intensity corrected in presence of YFP at the start of the imaging process (before bleaching) and I_{max} is the CFP intensity when CFP reaches its maximal recovery as YFP is totally bleached. Data are represented as mean ± SEM, and statistical analyses were done by using R software.

ACKNOWLEDGMENTS. We thank M. Jodar and S. Kouba for excellent technical assistance; F. Chatelain and T. Besson for oocyte recordings; S. Feliciangeli and A. Patel for proofreading of the manuscript; and A. Patel for the gift of TREK1 plasmids and S. Ducki for ML67. This work was supported by Fondation pour la Recherche Médicale via Equipe labellisée FRM 2011; the Agence Nationale de la Recherche's Laboratory of Excellence "Ion Channel Science and Therapeutics" Grant ANR-11-LABX-0015-01 and ANR blanche Dynaselect Grant ANR-14-CE13-0010); and the Basic Science Research Program through the National Research Foundation of Korea funded by the Ministry of Science, ICT, and Future Planning Grant NRF-2015R1A5A2008833.

1. Fink M, et al. (1996) Cloning, functional expression and brain localization of a novel unconventional outward rectifier K^+ channel. *EMBO J* 15(24):6854–6862.
2. Fink M, et al. (1998) A neuronal two P domain K^+ channel stimulated by arachidonic acid and polyunsaturated fatty acids. *EMBO J* 17(12):3297–3308.
3. Lesage F, Terrenoire C, Romey G, Lazdunski M (2000) Human TREK2, a 2P domain mechano-sensitive K^+ channel with multiple regulations by polyunsaturated fatty acids, lysophospholipids, and Gs, Gi, and Gq protein-coupled receptors. *J Biol Chem* 275(37):28398–28405.
4. Feliciangeli S, Chatelain FC, Bichet D, Lesage F (2015) The family of K2P channels: Salient structural and functional properties. *J Physiol* 593(12):2587–2603.
5. Devilliers M, et al. (2013) Activation of TREK-1 by morphine results in analgesia without adverse side effects. *Nat Commun* 4:2941.
6. Rodrigues N, et al. (2014) Synthesis and structure-activity relationship study of substituted caffeate esters as antinociceptive agents modulating the TREK-1 channel. *Eur J Med Chem* 75:391–402.
7. Marion E, et al. (2014) Mycobacterial toxin induces analgesia in buruli ulcer by targeting the angiotensin pathways. *Cell* 157(7):1565–1576.
8. Sandoz G, Levitz J, Kramer RH, Isacoff EY (2012) Optical control of endogenous proteins with a photoswitchable conditional subunit reveals a role for TREK1 in GABA(B) signaling. *Neuron* 74(6):1005–1014.
9. Xiao Z, et al. (2014) Activation of neurotensin receptor 1 facilitates neuronal excitability and spatial learning and memory in the entorhinal cortex: Beneficial actions in an Alzheimer's disease model. *J Neurosci* 34(20):7027–7042.
10. Borsotto M, et al. (2015) Targeting two-pore domain $K(^+)$ channels TREK-1 and TASK-3 for the treatment of depression: A new therapeutic concept. *Br J Pharmacol* 172(3):771–784.
11. Kennard LE, et al. (2005) Inhibition of the human two-pore domain potassium channel, TREK-1, by fluoxetine and its metabolite norfluoxetine. *Br J Pharmacol* 144(6):821–829.
12. Talley EM, Solorzano G, Lei Q, Kim D, Bayliss DA (2001) Cns distribution of members of the two-pore-domain (KCNK) potassium channel family. *J Neurosci* 21(19):7491–7505.
13. Yamamoto Y, Hatakeyama T, Taniguchi K (2009) Immunohistochemical colocalization of TREK-1, TREK-2 and TRAAK with TRP channels in the trigeminal ganglion cells. *Neurosci Lett* 454(2):129–133.
14. Kang D, Choe C, Kim D (2005) Thermosensitivity of the two-pore domain K^+ channels TREK-2 and TRAAK. *J Physiol* 564(Pt 1):103–116.
15. Kang D, Kim D (2006) TREK-2 (K2P10.1) and TRESK (K2P18.1) are major background K+ channels in dorsal root ganglion neurons. *Am J Physiol Cell Physiol* 291(1):C138–C146.
16. Noël J, et al. (2009) The mechano-activated K^+ channels TRAAK and TREK-1 control both warm and cold perception. *EMBO J* 28(9):1308–1318.
17. Pereira V, et al. (2014) Role of the TREK2 potassium channel in cold and warm thermosensation and in pain perception. *Pain* 155(12):2534–2544.
18. Brohawn SG, del Mármol J, MacKinnon R (2012) Crystal structure of the human K2P TRAAK, a lipid- and mechano-sensitive K+ ion channel. *Science* 335(6067):436–441.
19. Dong YY, et al. (2015) K2P channel gating mechanisms revealed by structures of TREK-2 and a complex with Prozac. *Science* 347(6227):1256–1259.
20. Lesage F, et al. (1996) Dimerization of TWIK-1 K+ channel subunits via a disulfide bridge. *EMBO J* 15(23):6400–6407.
21. Czirják G, Enyedi P (2002) Formation of functional heterodimers between the TASK-1 and TASK-3 two-pore domain potassium channel subunits. *J Biol Chem* 277(7): 5426–5432.
22. Blin S, et al. (2014) Tandem pore domain halothane-inhibited K^+ channel subunits THIK1 and THIK2 assemble and form active channels. *J Biol Chem* 289(41):28202–28212.
23. Hwang EM, et al. (2014) A disulphide-linked heterodimer of TWIK-1 and TREK-1 mediates passive conductance in astrocytes. *Nat Commun* 5:3227.
24. Veale EL, Rees KA, Mathie A, Trapp S (2010) Dominant negative effects of a non-conducting TREK1 splice variant expressed in brain. *J Biol Chem* 285(38):29295–29304.
25. Simkin D, Cavanaugh EJ, Kim D (2008) Control of the single channel conductance of K2P10.1 (TREK-2) by the amino-terminus: Role of alternative translation initiation. *J Physiol* 586(23):5651–5663.
26. Thomas D, Plant LD, Wilkens CM, McCrossan ZA, Goldstein SA (2008) Alternative translation initiation in rat brain yields K2P2.1 potassium channels permeable to sodium. *Neuron* 58(6):859–870.
27. Feliciangeli S, et al. (2010) Potassium channel silencing by constitutive endocytosis and intracellular sequestration. *J Biol Chem* 285(7):4798–4805.
28. Braun G, Lengyel M, Enyedi P, Czirják G (2015) Differential sensitivity of TREK-1, TREK-2 and TRAAK background potassium channels to the polycationic dye ruthenium red. *Br J Pharmacol* 172(7):1728–1738.
29. Enyedi P, Czirják G (2010) Molecular background of leak K^+ currents: Two-pore domain potassium channels. *Physiol Rev* 90(2):559–605.
30. Bagriantsev SN, et al. (2013) A high-throughput functional screen identifies small molecule regulators of temperature- and mechano-sensitive K2P channels. *ACS Chem Biol* 8(8):1841–1851.
31. Plant LD, Zuniga L, Araki D, Marks JD, Goldstein SA (2012) SUMOylation silences heterodimeric TASK potassium channels containing K2P1 subunits in cerebellar granule neurons. *Sci Signal* 5(251):ra84.
32. Shen NV, Chen X, Boyer MM, Pfaffinger PJ (1993) Deletion analysis of K^+ channel assembly. *Neuron* 11(1):67–76.
33. Fink M, et al. (1996) Dominant negative chimeras provide evidence for homo and heteromultimeric assembly of inward rectifier K^+ channel proteins via their N-terminal end. *FEBS Lett* 378(1):64–68.
34. Xu J, Yu W, Jan YN, Jan LY, Li M (1995) Assembly of voltage-gated potassium channels. Conserved hydrophilic motifs determine subfamily-specific interactions between the alpha-subunits. *J Biol Chem* 270(42):24761–24768.
35. Veale EL, et al. (2014) Influence of the N terminus on the biophysical properties and pharmacology of TREK1 potassium channels. *Mol Pharmacol* 85(5):671–681.
36. Murbartián J, Lei Q, Sando JJ, Bayliss DA (2005) Sequential phosphorylation mediates receptor- and kinase-induced inhibition of TREK-1 background potassium channels. *J Biol Chem* 280(34):30175–30184.
37. Patel AJ, et al. (1998) A mammalian two pore domain mechano-gated S-like K^+ channel. *EMBO J* 17(15):4283–4290.
38. Xiao Z, et al. (2009) Noradrenergic depression of neuronal excitability in the entorhinal cortex via activation of TREK-2 K^+ channels. *J Biol Chem* 284(16):10980–10991.
39. Chemin J, et al. (2003) Mechanisms underlying excitatory effects of group I metabotropic glutamate receptors via inhibition of 2P domain K^+ channels. *EMBO J* 22(20):5403–5411.
40. Van Munster EB, Kremers GJ, Adjobo-Hermans MJ, Gadella TW, Jr (2005) Fluorescence resonance energy transfer (FRET) measurement by gradual acceptor photobleaching. *J Microsc* 218(3)253–262.
41. Schneider CA, Rasband WS, Eliceiri KW (2012) NIH Image to ImageJ: 25 y of image analysis. *Nat Methods* 9(7):671–675.